Hindawi
Shock and Vibration
Volume 2020, Article ID 8304359, 21 pages
https://doi.org/10.1155/2020/8304359

Research Article

Effectiveness of Friction Dampers in Seismic and Wind Response Control of Connected Adjacent Steel Buildings

Anshul Malhotra, Tathagata Roy, and Vasant Matsagar

Multi-Hazard Protective Structures (MHPS) Laboratory, Department of Civil Engineering, Indian Institute of Technology (IIT) Delhi, Hauz Khas, New Delhi 110 016, India

Correspondence should be addressed to Vasant Matsagar; matsagar@civil.iitd.ac.in

Received 20 December 2019; Revised 25 July 2020; Accepted 6 August 2020; Published 15 September 2020

Academic Editor: Evgeny Petrov

Effectiveness of friction dampers (FDs) is investigated for connected dynamically similar and dissimilar steel buildings under uncorrelated seismic ground motion and wind excitations. The steel buildings involving moment-resisting frame (MRF) and braced frame (BF) are varied from five storeys to twenty storeys, which are connected by different configurations of the FDs. The steel buildings without and with bracing systems are modeled as plane frame structures with inertial masses lumped at each joint node. The FDs are modeled an element having yield force equal to slip load, with force-deformation behavior as elastic-perfectly plastic material. The dynamic responses of the unconnected and connected steel buildings are obtained in terms of top floor displacement and acceleration under the considered ground motion and wind excitations. It is concluded that the FDs help minimizing the gap between two adjacent buildings having utilized the space to connect the buildings. Moreover, the effectiveness of the FDs in terms of response reduction in dynamically dissimilar buildings is more than that in the similar buildings under the considered excitation scenarios. However, the effectiveness of the installed devices varies significantly under the multiple loading scenarios. Finally, the separation gap may be reduced by ~30%, which would eventually minimize structural pounding as well as utilize the space for effective construction. Hence, important essential guidelines are outlined for structures installed with such passive control devices against such multiple scenario loadings.

1. Introduction

Structures constructed in moderate-to-high seismicity and windy regions have experienced damages due to extreme vibrational effects under severe ground shaking and gusty wind loading imparted [1–6]. To minimize these damaging effects and improve the behavior of the structures under such dynamic excitations, friction damper (FD) has been one of the potential passive response control devices developed in minimizing the large response of a structure under the extreme earthquake and wind excitations [7, 8]. In a typical FD, the generated frictional force helps to dissipate the external energy and stabilize the structure under the dynamic excitation scenarios [9]. The FDs are also not prone to thermal effects and possess a stable hysteretic behavior for a considerable number of cycles under such dynamic excitations [10]. Moreover, the FDs have a reliable performance under the dynamic excitations as compared to the other conventional methods and their installation and maintenance are relatively simple. Therefore, these advantages make the FDs a suitable choice for design of new structures as well as rehabilitation and strengthening of existing structures to achieve safety of the structures under the multiple catastrophic seismic and wind hazards [11, 12].

With the recent increase in urbanization and globalization, the structural engineers and designers are enforced to construct buildings at a close vicinity resulting in insufficient separation gap between the buildings. Such insufficient gap leads to structural pounding under the effects of seismic ground motions and gusty winds, which may lead to catastrophic collapse of the buildings, as observed during 1985 Mexico City earthquake. The primary reason of impact

between the adjacent buildings under the effects of earthquake (or wind excitations) is the difference in their dynamic properties. These differences in structural properties lead to out-of-phase vibrations causing structural pounding, which warrants technical knowhow for constructions in high-urbanized regions across the world [13]. Hence, in order to have effective utilization of the space between two structures, coupling of the adjacent structures with suitable control mechanisms becomes an effective solution to reduce the overall responses of the building systems under the effects of earthquake and wind excitations [14].

The friction damper (FD) was initially used in steel buildings for improving the seismic performance [15, 16]. The proposed device was helpful to upgrade the seismic resistance of the existing building frames. Thereafter, the FDs were adopted for braced frames, buildings with shear walls, and low-rise buildings to mitigate the large deformations caused by earthquake ground motions and winds [17–19]. The application of this novel structural system was further focused on construction of an 18-storey steel apartment building in India [20]. It was observed that significant seismic response reduction was achieved on application of the Pall FDs in the steel building. Research further progressed in assessing and designing the parameters of the FDs for different structural systems under ground motion excitations [10, 21]. Lately, the FDs were used in mid-rise to high-rise buildings along with diagonal bracing, which reduced the seismic responses considerably [22, 23]. Moreover, Montuori et al. [24] presented an innovative approach to design a seismic resistant system for the combination of moment-resisting frame (MRF) and a bracing system installed with the FDs. Thereafter, multiobjective optimization procedure was applied to find the optimal placements of the FDs in building frame [25–27]. Research is also conducted to optimize the slip load and investigate the hysteretic behavior of structures using rotational FD [28, 29]. The FD has also found its application in the infrastructure system, such as transmission tower to control the large seismic deformations [30].

Coupling of adjacent buildings has been an emerging technique to mitigate the large structural responses due to wind and seismic excitations [31, 32]. The concept allows two dynamically similar and/or dissimilar structures to exert the forces upon one another for overall response reduction of the system. The available studies showed improved performance of the structural systems by connecting different passive control devices to limit the pounding actions under earthquake ground motions [14, 33–39]. Overall, the FDs have offered its potential in minimizing the extreme vibrations installed in a structure; however, research strategies have not been implemented to assess the response and quantify the effectiveness of the FDs for coupled adjacent buildings under both seismic and wind excitations. Therefore, it becomes important to investigate the connected structures installed with the FDs to mitigate the responses of adjoining building and avoiding poundings against the multihazard scenario of earthquake and wind loadings during design life of structures.

Herein, effectiveness of the FDs is investigated for connected dynamically similar and dissimilar adjacent steel moment-resisting frame (MRF) and braced frame (BF) buildings with varying storeys under the multihazard uncorrelated scenarios of seismic and wind hazards. Site-specific earthquake ground motions and wind excitations are assumed to describe the multihazard scenario for assessment of the unconnected and connected steel structures. In view of the abovementioned gaps, the main objectives of the current study are as follows: (i) to study the effectiveness of the FDs for the connected dynamically similar and dissimilar multistorey buildings under multihazard earthquake and wind excitations and (ii) to investigate the effects of varying number of storeys of the connected dynamically similar and dissimilar multistorey buildings under earthquake and wind excitations evaluating the response of the FDs in multihazard conditions.

2. Mathematical Modeling

Mathematical models for N-storey dynamically similar and dissimilar moment-resisting frames (MRFs) and braced frames (BFs) connected by the FDs are developed for different configurations, as shown in Figures 1 and 2, under the dynamic earthquake and wind loadings. Three configuration systems for the connected buildings, viz., configuration A, B, and C are considered to assess the effectiveness of the FDs. Configuration A has two friction dampers at each storey in X crossing pattern, with cross-bracing at all floor levels, as shown in Figures 1(c) and 2(c). Configuration B has one friction damper at each storey in a zigzag pattern as shown in Figures 1(d) and 2(d). Configuration C has two friction dampers at each storey in X crossing pattern up to $0.4N$ of upper storey of the building from the top, as shown in Figures 1(e) and 2(e), where N is the number of storey. The assumptions made for developing the mathematical models are as follows: (i) the building members except the FDs are assumed to remain in the elastic limit, a design decision in structural control, (ii) one degree of freedom (DOF) at each floor level in the direction of earthquake ground motion and wind is considered, (iii) the inertial mass is lumped at each floor level, (d) the floors are assumed to be rigid in their own plane, and (e) strength degradation of friction dampers is presently ignored in the analysis.

2.1. Moment-Resisting Frame (MRF). The governing differential equation of motion for the MRF, in general, is written as

$$[M]\{\ddot{u}(t)\} + [C]\{\dot{u}(t)\} + [K]\{u(t)\} = F(t), \tag{1}$$

where $[M]$, $[C]$, and $[K]$ are the mass, damping, and stiffness matrices of the primary structure, respectively. Moreover, $\{\ddot{u}(t)\}$, $\{\dot{u}(t)\}$, and $\{u(t)\}$ are the acceleration, velocity, and displacement response of the primary structure, respectively. Furthermore, $F(t)$ is the external force exerted on the structure, either during the earthquake or wind event. Here, $F(t) = -[M]\{r\}\{\ddot{u}_g(t)\}$ is the inertial force vector induced because of the earthquake ground motion applied to the

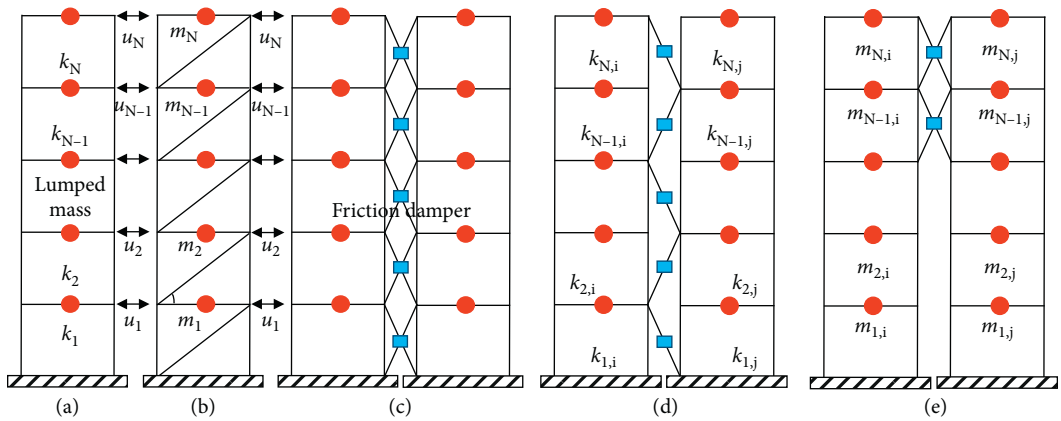

FIGURE 1: Mathematical models of N-storey: (a) unconnected (U) moment-resisting frame (MRF), (b) unconnected (U) braced frame (BF), (c) connected frames (configuration A), (d) connected frames (configuration B), and (e) connected frames (configuration C) for equal storey height.

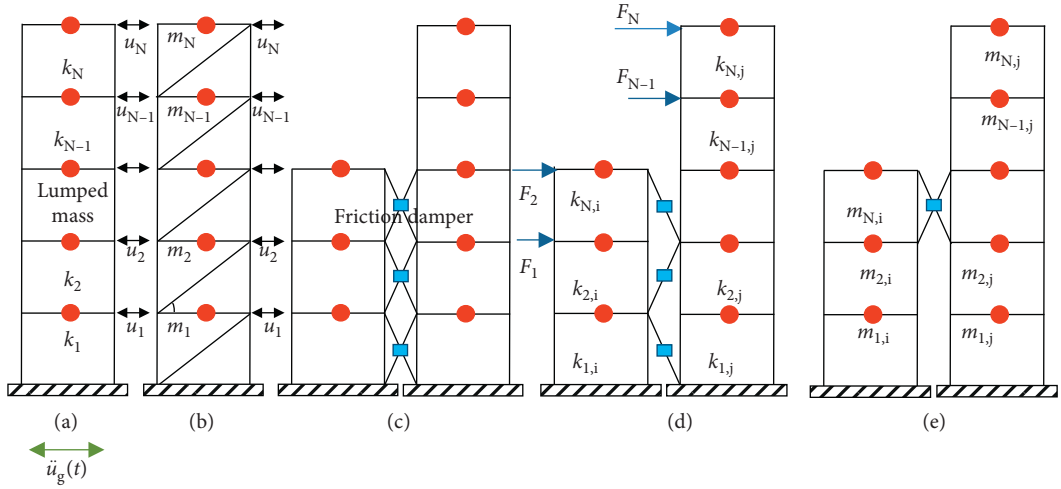

FIGURE 2: Mathematical models of N-storey: (a) unconnected (U) moment-resisting frame (MRF), (b) unconnected (U) braced frame (BF), (c) connected frames (configuration A), (d) connected frames (configuration B), and (e) connected frames (configuration C) for unequal storey heights.

structure (base-excited structure), or $F(t) = \{F_1, F_2, F_3, \ldots, F_n\}^T$ is the applied wind force vector at the floor mass on each storey (mass-excited structure). Here, the earthquake ground acceleration is denoted by $\ddot{u}_g(t)$ and $\{r\}$ is the influence coefficient vector. The wind force, $F_n(t) = 0.5\rho C_d A(V+\Delta v)^2$, depends on the environment and building conditions, such as, density of air, ρ; coefficient of drag, C_d; depending on shape of the building; area of wind load exposure for n^{th} floor, A_n; mean wind speed, V; and fluctuating wind component, Δv. For the MRF, the structure is defined by its mass matrix, damping matrix, and stiffness matrix as $[M]$, $[C]$, and $[K]$, respectively. Here, $[M]$ is a diagonal matrix with the diagonal element $m_{jj} = m_j$, the mass lumped at the j^{th} floor. Flexural rigidity of the columns provides lateral force resistance in the MRF; therefore, only column stiffness contributes towards the formation of $[K]$ matrix. The mass and stiffness matrix of the N-storey MRF can be given as

$$[M] = \begin{bmatrix} m_1 & 0 & 0 & \cdots & 0 & 0 \\ 0 & m_2 & 0 & \cdots & 0 & 0 \\ 0 & 0 & m_3 & \cdots & 0 & 0 \\ \vdots & \vdots & \vdots & \ddots & \vdots & \vdots \\ 0 & 0 & 0 & \cdots & m_{N-1} & 0 \\ 0 & 0 & 0 & \cdots & 0 & m_N \end{bmatrix}, \quad (2)$$

$$[K] = \begin{bmatrix} k_1 + k_2 & -k_2 & 0 & \cdots & 0 & 0 \\ -k_2 & k_2 + k_3 & -k_3 & \cdots & 0 & 0 \\ 0 & -k_3 & k_3 + k_4 & \cdots & 0 & 0 \\ \vdots & \vdots & \vdots & \ddots & \vdots & \vdots \\ 0 & 0 & 0 & \cdots & k_{N-1} + k_N & -k_N \\ 0 & 0 & 0 & \cdots & -k_N & k_N \end{bmatrix}. \quad (3)$$

2.2. Braced Frame (BF). The governing differential equation of motion for the BF is written as

$$[M]\{\ddot{u}(t)\} + [C]\{\dot{u}(t)\} + \left([K] + [K_b]\cos^2\theta\right)\{u(t)\} = F(t), \tag{4}$$

where $[M]$ and $[C]$ matrices are constructed similar as that in case of the MRF. In the BF, stiffness of the structure is the combined effect of the stiffness imparted by the columns, i.e., $[K]$, and the braces, i.e., $[K_b]$. Here, θ_N is the angle of the brace with horizontal at the N^{th} storey level and $k_{bi} = k_{b1}, k_{b2}, k_{b3} \ldots k_{bN}$ denote the axial stiffness of the braces:

$$[K_b] = \begin{bmatrix} k_{b1}+k_{b2} & -k_{b2} & 0 & \cdots & 0 & 0 \\ -k_{b2} & k_{b2}+k_{b3} & -k_{b3} & \cdots & 0 & 0 \\ 0 & -k_{b3} & k_{b3}+k_{b4} & \cdots & 0 & 0 \\ \vdots & \vdots & \vdots & \ddots & \vdots & \vdots \\ 0 & 0 & 0 & \cdots & k_{b(N-1)}+k_{bN} & -k_{bN} \\ 0 & 0 & 0 & \cdots & -k_{bN} & k_{bN} \end{bmatrix}. \tag{5}$$

In the BF, the braces are assumed to carry only the axial force and the brace sections are so chosen to ensure that they do not buckle under compression and do not yield under tension.

2.3. Connected Frame Using Friction Damper (FD). Coulomb's dry friction is used to model the nonlinear behavior of the FDs. The nonlinearity is concentrated only in the friction dampers, assuming rest of the building members (the primary structural system) is in elastic range. This is done to ensure that the energy dissipation occurs in friction dampers only and not by yielding of any other structural members. Hence, the structures with the FDs can be treated as a dual system consisting of nonlinear energy-dissipating devices exhibiting elastoplastic behavior and a primary structural system exhibiting linear behavior. Based on this assumption, the governing equation of motion can be written as

$$\left[M_{eff}\right]\{\ddot{u}(t)\} + \left(\left[C_{eff}\right]\right)\{\dot{u}(t)\} + \left[K_{eff}\right]\{u(t)\} + F_d = F(t), \tag{6}$$

where $C_{eff} = C + C_d$ and $K_{eff} = K + K_d$. C is the equivalent damping of the building systems, and C_d is the equivalent damping of the FD. Similarly, K is the equivalent stiffness of the building systems and K_d is the equivalent stiffness of the FD, which is assumed to be zero here. $F_d(t) = \mu m_N g \operatorname{sgn}(\dot{u})$ is the frictional force exerted by the FD under the earthquake or wind load, and $m_N g$ or W is the slip load for the FD at each storey level, with g denoting the acceleration due to gravity. The matrices for equation (6) are discussed as follows:

$$\left[M_{eff}\right] = \begin{bmatrix} M_A & 0 \\ 0 & M_B \end{bmatrix}, \tag{7}$$

$$[M_A] = \begin{bmatrix} m_{1A} & 0 & 0 & \cdots & 0 & 0 \\ 0 & m_{2A} & 0 & \cdots & 0 & 0 \\ 0 & 0 & m_{3A} & \cdots & 0 & 0 \\ \vdots & \vdots & \vdots & \ddots & \vdots & \vdots \\ 0 & 0 & 0 & \cdots & m_{P-1,A} & 0 \\ 0 & 0 & 0 & \cdots & 0 & m_{P,A} \end{bmatrix}, \tag{8}$$

$$[M_B] = \begin{bmatrix} m_{1B} & 0 & 0 & \cdots & 0 & 0 \\ 0 & m_{2B} & 0 & \cdots & 0 & 0 \\ 0 & 0 & m_{3B} & \cdots & 0 & 0 \\ \vdots & \vdots & \vdots & \ddots & \vdots & \vdots \\ 0 & 0 & 0 & \cdots & m_{Q-1,B} & 0 \\ 0 & 0 & 0 & \cdots & 0 & m_{Q,B} \end{bmatrix}, \tag{9}$$

$$\left[K_{eff}\right] = \begin{bmatrix} K_A & 0 \\ 0 & K_B \end{bmatrix}, \tag{10}$$

$$K_A = \begin{bmatrix} k_{11,A}+k_{21,A} & -k_{21,A} & 0 & \cdots & 0 & 0 \\ -k_{21,A} & k_{21,A}+k_{31,A} & k_{21,A}+k_{31,A} & \cdots & 0 & 0 \\ 0 & -k_{31,A} & k_{31,A}+k_{41,A} & \cdots & 0 & 0 \\ \vdots & \vdots & \vdots & \ddots & \vdots & \vdots \\ 0 & 0 & 0 & \cdots & k_{P-11,A}+k_{P1,A} & -k_{P1,A} \\ 0 & 0 & 0 & \cdots & -k_{P1,A} & k_{P1,A} \end{bmatrix}, \tag{11}$$

$$K_B = \begin{bmatrix} k_{11,B} & -k_{21,B} & 0 & \cdots & 0 & 0 \\ -k_{21,B} & k_{21,B}+k_{31,B} & -k_{31,B} & \cdots & 0 & 0 \\ 0 & -k_{31,B} & k_{31,B}+k_{41,B} & \cdots & 0 & 0 \\ \vdots & \vdots & \vdots & \ddots & \vdots & \vdots \\ 0 & 0 & 0 & \cdots & k_{Q-11,B}+k_{Q1,B} & -k_{Q1,B} \\ 0 & 0 & 0 & \cdots & -k_{Q1,B} & k_{Q1,B} \end{bmatrix}, \tag{12}$$

$$\left[C_{eff}\right] = \begin{bmatrix} C_A & 0 \\ 0 & C_B \end{bmatrix}, \tag{13}$$

$$[C_A] = \begin{bmatrix} c_{11,A}+c_{21,A} & -c_{21,A} & 0 & \cdots & 0 & 0 \\ -c_{21,A} & c_{21,A}+c_{31,A} & -c_{31,A} & \cdots & 0 & 0 \\ 0 & -c_{31,A} & c_{31,A}+c_{41,A} & \cdots & 0 & 0 \\ \vdots & \vdots & \vdots & \ddots & \vdots & \vdots \\ 0 & 0 & 0 & \cdots & c_{P-11,A}+c_{P1,A} & -c_{P1,A} \\ 0 & 0 & 0 & \cdots & -c_{P1,A} & c_{P1,A} \end{bmatrix}, \tag{14}$$

$$[C_B] = \begin{bmatrix} c_{11,B}+c_{21,B} & -c_{21,B} & 0 & \cdots & 0 & 0 \\ -c_{21,B} & c_{21,B}+c_{31,B} & -c_{31,B} & \cdots & 0 & 0 \\ 0 & -c_{31,B} & c_{31,B}+c_{41,B} & \cdots & 0 & 0 \\ \vdots & \vdots & \vdots & \ddots & \vdots & \vdots \\ 0 & 0 & 0 & \cdots & c_{Q-11,B}+c_{Q1,B} & -c_{Q1,B} \\ 0 & 0 & 0 & \cdots & -c_{Q1,B} & c_{Q1,B} \end{bmatrix}, \tag{15}$$

$$[C_d] = \begin{bmatrix} [C_d] & 0 & [-C_d] \\ 0 & 0 & 0 \\ [-C_d] & 0 & [C_d] \end{bmatrix}, \tag{16}$$

$$[C_d] = \begin{bmatrix} c_{d1} & 0 & 0 & \cdots & 0 & 0 \\ 0 & c_{d2} & 0 & \cdots & 0 & 0 \\ 0 & 0 & c_{d1} & \cdots & 0 & 0 \\ \vdots & \vdots & \vdots & \ddots & \vdots & \vdots \\ 0 & 0 & 0 & \cdots & c_{d,N-1} & 0 \\ 0 & 0 & 0 & \cdots & 0 & c_{d,N} \end{bmatrix}. \tag{17}$$

Moreover, $F_d(t) = \mu m_N g \mathrm{sgn}(\dot{u})$ is the frictional force exerted by the FD under the earthquake or wind load, and $m_N g$ or W is the slip load for the FD at each storey level, with g denoting the acceleration due to gravity. Figure 3 shows the force-deformation behavior of the FD assumed for this study. Furthermore, the stiffness of the brace of the FD is neglected; however, considering realistically the force-deformation behavior of the friction damper does include initial stiffness provided by the brace.

The numerical solution of the governing differential equations given above for the MRF and BF connected by the FD are obtained by using Newmark's method of nonlinear modal time history adopting linear variation of acceleration over an interval of Δt. The time interval for solving the

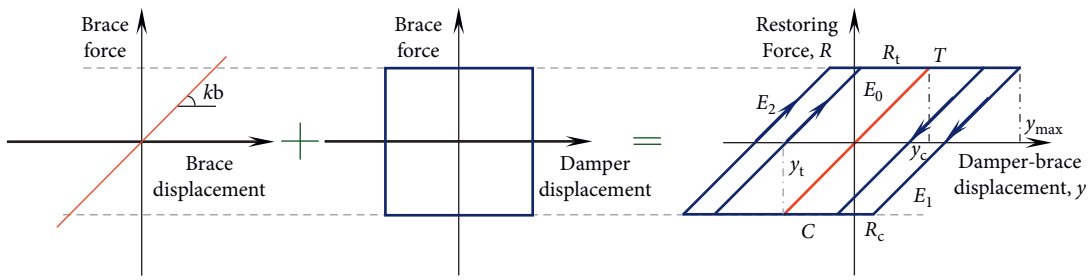

Figure 3: (a) Elastic behavior of brace, (b) hysteretic loop of friction damper, and (c) resultant elastoplastic behavior of the friction damper in brace.

Table 1: Modeling properties of the elastic-plastic friction damper (FD).

Properties of friction damper	Values
Effective stiffness	0
Stiffness	$5000k$, k is the stiffness of each storey
Yield strength	0.3 W, W is the storey weight
Postyield stiffness ratio	1×10^{-6}
Yielding coefficient	20

equations of motion is taken as Δt, which also depends on the time step for the external load applied (earthquake ground motion or gusty wind loading).

3. Multihazard Scenario under Earthquake and Wind Excitations

The multihazard assessment strategy involves proper selection of hazard models to assess a structure under the effects of earthquake and wind loadings in a region [40]. The hazard models may be generated using empirical equations, spectra established on physical models, or adopting the already available data from the past earthquake or wind events recorded at the nearest station. For the present study, actual time history data of the earthquake from a recorded station and synthesized time history data of the wind loading from the same region are assumed to investigate the effectiveness of the FD when used to connect adjacent buildings. The time history data are chosen for two different regions, viz., California region of the United States of America (USA), and Kobe city in the southeast region of Japan. The locations are carefully chosen in such a way that the probability of occurrence of the multiple hazards is considerably higher than other regions of the world. Moreover, the considered earthquakes have caused extreme devastations to socioeconomic life as observed from the global statistics. The wind loads, with static and fluctuating components, are simulated from the NatHaz online wind simulator (NOWS): simulation of Gaussian multivariate wind fields [41]. The simulation technique involves obtaining discrete frequency function with Cholesky decomposition and fast Fourier transform (FFT) for wind speed, which is considered as the wind hazard parameter here. The time histories of the wind speeds are obtained thence by summing the static and the fluctuating components obtained from the simulation based on Bernoulli's theorem.

4. Numerical Study

Herein, a numerical study is conducted to evaluate the effectiveness of the FDs for the connected steel MRF and BF buildings. Modal damping of $\xi = 2\%$ is considered for the two steel buildings. The normalized slip load for the FD at each storey level considered for the study is assumed 30% of the storey weight (W), which can suitably be optimized otherwise. The other relevant parameters adopted to model the FDs for the connected steel buildings are shown in Table 1. For further study, the variation of height is considered in 5, 10, 15, and 20 storey for dynamically similar and dissimilar building frames connected by the FDs. Free vibration analysis is conducted to obtain the modal responses for the unconnected MRFs and BFs, and the results are shown in Table 2. Four historical earthquake ground motions and synthesized wind excitations are selected for the numerical study, for which the details are given in Tables 3 and 4. The response spectrum of ground motion acceleration and displacement is plotted for the selected earthquakes to demonstrate the nature of the responses obtained for the steel buildings, as shown in Figure 4. The wind hazard incorporated in the study is simulated from the NatHaz online simulator with gust speed as 30 m/s, 37 m/s, 43 m/s, and 50 m/s located in urban and suburban areas with numerous closely spaced obstructions (category-B) having cutoff frequencies obtained from the free vibration analysis of the building frames. The gust wind speeds are noted from the regions of interest where multiple hazard scenarios exist. Time history of the wind excitation for different gust speeds along with the corresponding fast Fourier transform (FFT) for the steel buildings is plotted in Figure 5. The FFT spectrum refers to the frequency in the considered wind loads, essential in evaluating the nature of the structural

Table 2: Modal periods of the unconnected steel MRF and BF structures.

Building type	Modal periods		
	First	Second	Third
5-storey MRF	0.54	0.18	0.12
10-storey MRF	1.02	0.34	0.21
15-storey MRF	1.51	0.51	0.31
20-storey MRF	1.90	0.63	0.38
5-storey BF	0.32	0.11	0.07
10-storey BF	0.62	0.21	0.13
15-storey BF	0.91	0.31	0.18
20-storey BF	1.15	0.38	0.23

Table 3: Details of the earthquake ground motion.

Sl. No.	Earthquake	Year	Recording station	Component	PGA (g)
1	Imperial Valley	1940	El Centro	S00 E	0.34
2	Loma Prieta	1989	LGPC	N00 E	0.56
3	Northridge	1994	Rinaldi	N360S	0.83
4	Kobe	1995	JMA Record	EW	0.67

Table 4: Details of the wind time history.

Sl. No.	Wind speed (m/s)	Cutoff frequency (Hz)	Exposure category	Duration (s)
1	30	0.5	B	3000
2	37			
3	43			
4	50			

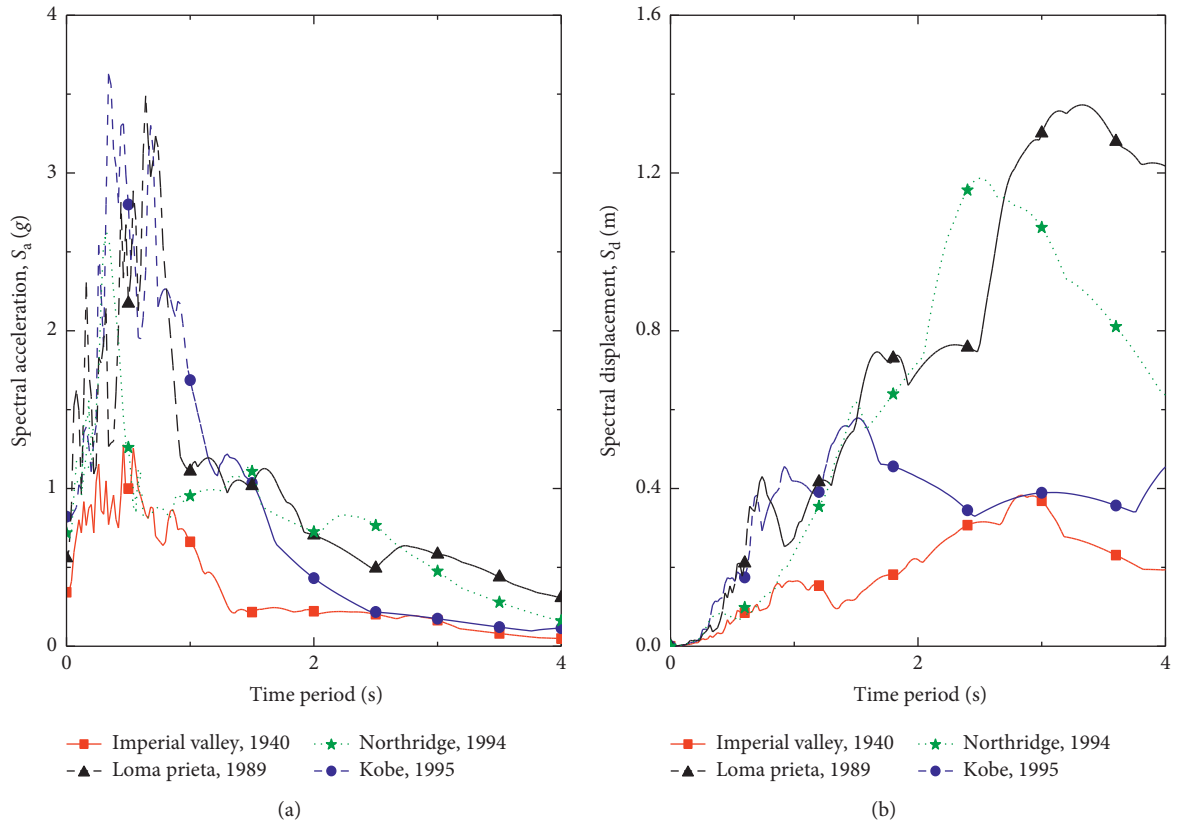

Figure 4: Acceleration and displacement response spectra of the considered historical earthquake ground motions.

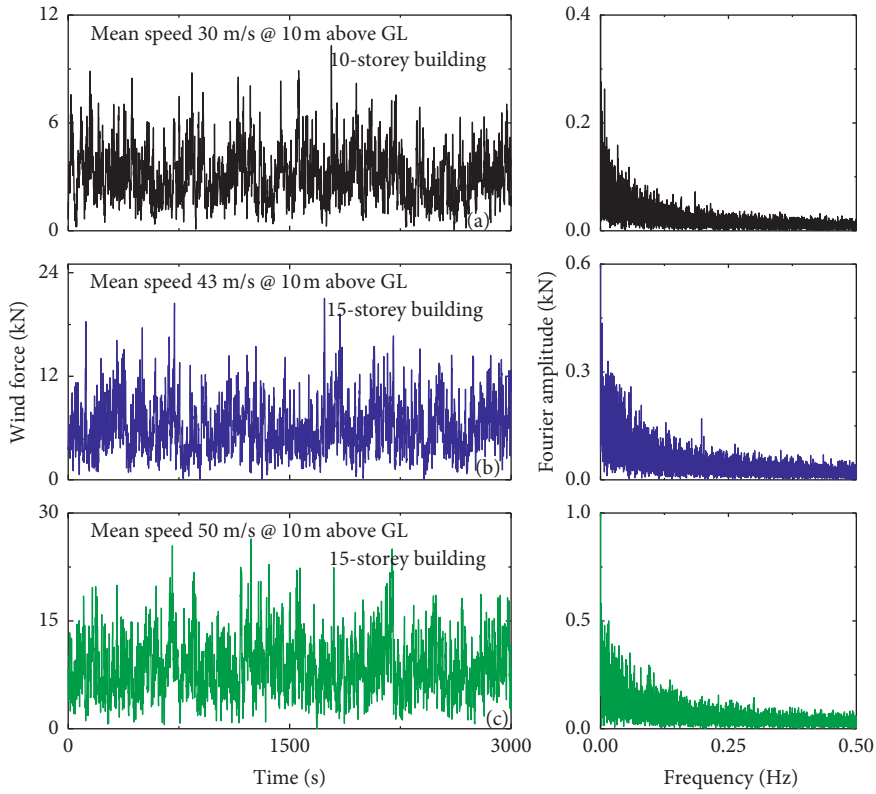

Figure 5: Wind speed at specific height for 10- and 15-storey buildings along with the frequency content (FFT spectra).

Table 5: Combinations of dynamically similar and dissimilar connected buildings considered for the study.

Similar buildings		Dissimilar buildings			
MRF*-MRF	BF*-BF	MRF*-BF	BF*-MRF	MRF*-MRF	BF*-BF
5-5	5-5	5-5	5-5	5-10	5-10
10-10	10-10	10-10	10-10	5-15	5-15
15-15	15-15	15-15	15-15	5-20	5-20
20-20	20-20	20-20	20-20	10-15	10-15
—	—	—	—	10-20	10-20
—	—	—	—	15-20	15-20

*Responses shown for that particular building.

responses under the gusty wind loads. The top floor displacement (u_n, $n = 5$, 10, 15, or 20) and acceleration ($\ddot{u}_n$, $n = 5$, 10, 15, or 20) of dynamically similar and dissimilar unconnected buildings are compared with the connected buildings to evaluate the effectiveness and to obtain the best suitable configuration of the FDs. Note, hence on the peak top floor displacement is denoted by x_n; whereas, the peak top floor acceleration is denoted by $\ddot{x}_n$. The connected structures considered in the study are as follows: (a) MRF-MRF, (b) BF-BF, (c) MRF-BF, (d) BF-MRF, (e) different storeys for MRF-MRF, and (f) different storeys for BF-BF, also summarized in Table 5, which constitutes of the most prominent configurations of the buildings. The direction of loading, earthquake or wind, is applied in the direction of left to right of the shear frames, i.e., along the degree of freedom (DOF) considered at the lumped masses. The wind load is applied from 10 m above ground level at the center of mass of the structure, as shown in Figure 2(d). The direction of wind load has no contribution to the objective of the study, rather it is just a choice of analysis procedure. Finally, the buildings are connected by the FDs keeping 5 m separation gap distance, as recommended by most of the building bylaws across the world.

4.1. Effectiveness of FD for Dynamically Similar Connected Buildings. Herein, the effectiveness of the FDs is investigated by comparing the responses of the unconnected (U) and connected (C) steel MRFs and BFs for different configurations of the passive FD under earthquake ground motions and wind forces. The responses are illustrated in terms of time history plots under the considered loading scenarios to demonstrate the effectiveness of the FDs. Moreover, peak responses are plotted to understand the variation in the responses for the considered connected buildings obtained under the dynamic loading scenarios.

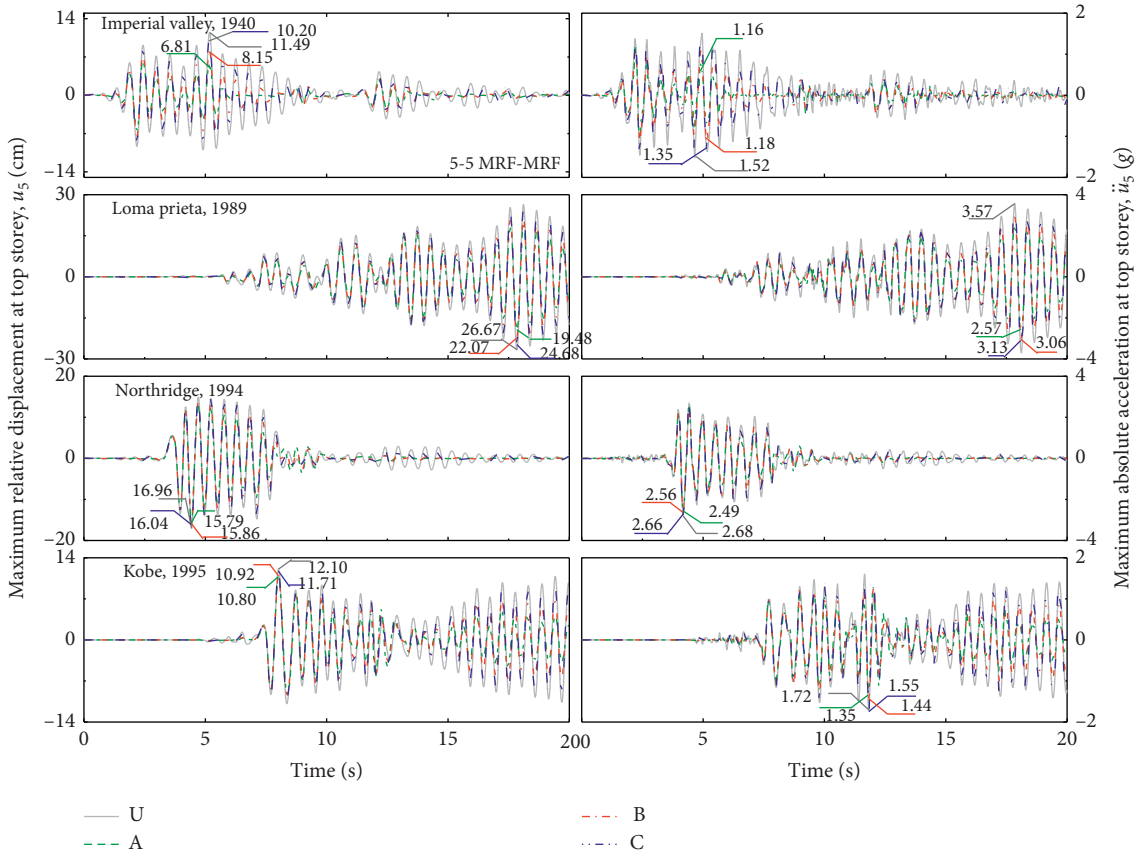

(a)

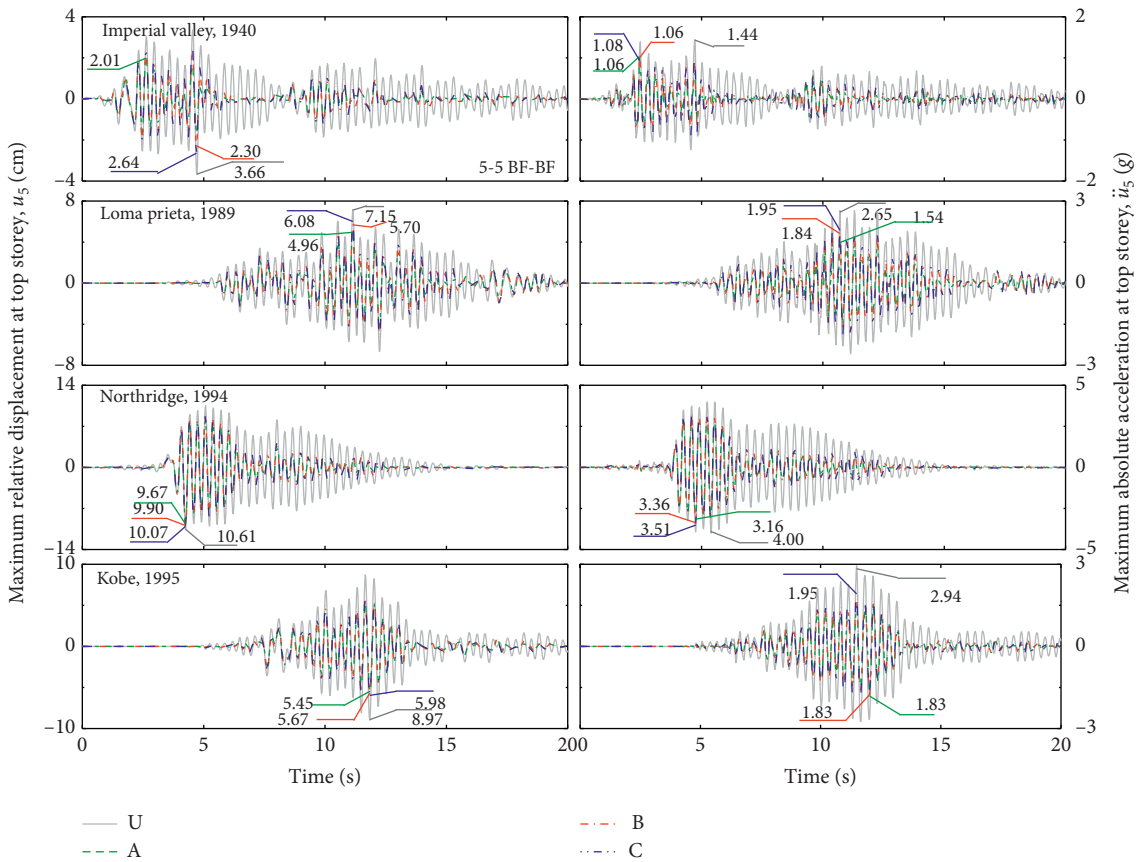

(b)

Figure 6: (a) Time history response of top floor displacement and acceleration of connected steel 5-5 MRF-MRF buildings under different earthquake ground motions. (b) Time history response of top floor displacement and acceleration of connected steel 5-5 BF-BF buildings under different earthquake ground motions.

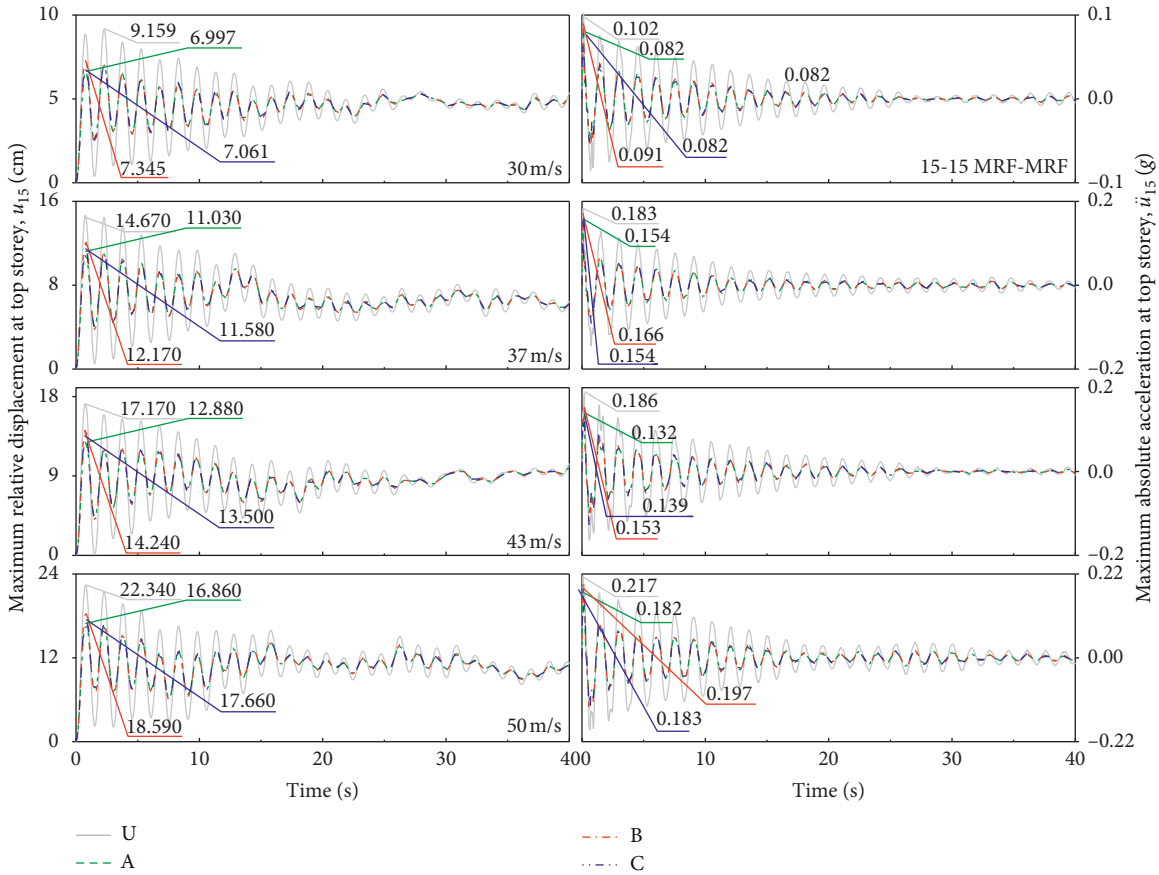

FIGURE 7: Time history response of top floor displacement and acceleration of connected steel 15-15 MRF-MRF buildings under different wind gust speeds.

Figures 6(a) and 6(b) show the displacement and acceleration responses in time history scale for the dynamically similar connected 5-storey MRF and BF under the considered earthquake ground excitations, whereas Figure 7 shows the dynamic responses of the connected 15-storey MRF under the considered wind forces.

Considering top floor displacement, the reduction in peak response for 5-5 MRF-MRF when connected using configuration A is obtained from ~7% to 41%, whereas the reduction is, respectively, obtained from 6% to 29% and ~3% to 11% for configurations B and C under the historical earthquakes. Furthermore, for the top floor acceleration, the response reductions for configurations A, B, and C are, respectively, obtained from ~7% to 28%, ~4% to 22%, and ~1% to 7%. Similar observations are also noted for the 5-5 BF-BF. Hence, the FDs used in configuration A are able to dissipate the highest amount of induced input energy as compared to the other configuration of FDs. For the considered wind loads, 15-storey connected MRF is studied, and it is observed that the reduction in the peak top floor displacement is also the highest for configuration A (~23% to 25%) as compared to configurations B (~17% to 20%) and C (~21% to 23%). However, the range of difference under the wind loads is quite small as compared to the range under the earthquakes. For the peak top floor acceleration, the highest response reduction is also obtained for configuration A (~16% to 29%), whereas the least response reduction is observed under configuration B under both earthquake and wind loads.

Similarly, the displacement and acceleration responses for all the considered dynamically similar buildings with increased storey heights under earthquakes and winds are compared from Tables 6 and 7 as well as from Figures 8(a) and 8(b). Overall, under the earthquake excitations, the response reduction for top floor displacement and acceleration of the low-rise buildings is significantly higher as compared to high-rise buildings, which is observed to be contrary for the wind scenario that has increased response reduction for high-rise buildings. The characteristics of the obtained dynamic responses depend mainly on the modal properties of the structure and nature of the dynamic excitations. The displacement responses for the dynamically similar connected buildings under the earthquakes and winds increase with increase in building height. Moreover, the displacement responses obtained under the earthquakes increased significantly as compared to the responses obtained under the wind loadings. This implies that the energy content of the earthquake is comparably higher and has significant effect in determining the responses of the structure. On the other hand, the acceleration responses for the dynamically similar connected buildings under the earthquakes decrease with increase in building height. Conversely, the acceleration responses

Table 6: Peak top floor displacement and acceleration responses of similar connected buildings for equal storey height under historical earthquake ground motions.

Frame	Earthquake	Peak top floor displacement, x_n (cm)				Peak top floor acceleration, $\ddot{x}_n$ (g)			
		U	A	B	C	U	A	B	C
5-5 MRF-MRF	Imperial Valley, 1940	11.49	6.81	8.15	10.20	1.52	1.16	1.18	1.35
	Loma Prieta, 1989	26.67	19.48	22.07	24.68	3.57	2.57	3.06	3.13
	Northridge, 1994	16.96	15.79	15.86	16.04	2.68	2.49	2.56	2.66
	Kobe, 1995	12.10	10.80	10.92	11.71	1.72	1.35	1.44	1.55
20-20 MRF-MRF	Imperial Valley, 1940	22.18	15.82	19.24	21.81	0.59	0.43	0.45	0.51
	Loma Prieta, 1989	81.23	59.32	68.11	73.82	2.10	1.74	1.81	1.86
	Northridge, 1994	81.67	72.70	76.64	78.10	1.63	1.53	1.54	1.58
	Kobe, 1995	37.41	30.32	35.72	36.78	1.31	1.12	1.24	1.29
5-5 BF-BF	Imperial Valley, 1940	3.66	2.01	2.30	2.64	1.44	1.06	1.06	1.08
	Loma Prieta, 1989	7.15	4.96	5.70	6.08	2.65	1.54	1.84	1.95
	Northridge, 1994	10.61	9.67	9.90	10.07	4.00	3.16	3.36	3.51
	Kobe, 1995	8.97	5.45	5.67	5.98	2.94	1.83	1.83	1.95
20-20 BF-BF	Imperial Valley, 1940	15.72	7.21	10.58	12.74	0.77	0.60	0.65	0.71
	Loma Prieta, 1989	46.08	35.28	42.91	44.81	1.86	1.60	1.75	1.80
	Northridge, 1994	40.27	29.97	34.87	36.71	2.25	1.94	2.15	2.15
	Kobe, 1995	33.50	27.11	27.53	28.55	2.08	1.74	1.89	1.94

Table 7: Peak top floor displacement and acceleration responses of similar connected buildings for equal storey height under simulated wind forces for different gust speeds.

Frame	Wind speed (m/s)	Peak top floor displacement, x_n (cm)				Peak top floor acceleration, $\ddot{x}_n$ (g)			
		U	A	B	C	U	A	B	C
5-5 MRF-MRF	30	1.74	1.74	1.74	1.74	0.10	0.097	0.10	0.10
	37	2.16	2.16	2.16	2.16	0.24	0.24	0.24	0.25
	43	3.87	3.66	3.76	3.72	0.39	0.38	0.38	0.38
	50	3.90	3.69	3.69	3.69	0.30	0.29	0.29	0.29
20-20 MRF-MRF	30	25.74	16.74	18.74	17.74	0.23	0.15	0.17	0.16
	37	28.16	19.16	20.16	19.88	0.35	0.234	0.264	0.25
	43	32.87	21.66	23.76	22.82	0.42	0.27	0.31	0.29
	50	37.90	24.69	28.69	26.69	0.48	0.32	0.35	0.32
5-5 BF-BF	30	0.23	0.23	0.23	0.23	0.039	0.039	0.03	0.039
	37	0.29	0.29	0.29	0.29	0.093	0.093	0.09	0.093
	43	0.52	0.51	0.51	0.51	0.15	0.15	0.15	0.15
	50	0.50	0.50	0.50	0.50	0.094	0.093	0.094	0.093
20-20 BF-BF	30	4.09	3.31	3.60	3.42	0.064	0.059	0.061	0.060
	37	5.69	4.61	5.01	4.75	0.098	0.081	0.088	0.082
	43	6.75	5.47	5.94	5.64	0.12	0.098	0.11	0.10
	50	8.95	7.25	7.88	7.48	0.14	0.12	0.12	0.12

obtained under the wind loadings increases with increase in building height, thus demonstrating the influence of acceleration as a design parameter for high-rise structures. Therefore, installation of such passive device to minimize structural response under a particular hazard may not necessarily yield satisfactory performance under the other hazard, which becomes a possible example of a multi-hazard situation wherein careful selection of the design parameters for such structures is a necessity for modern constructions in the regions where such multihazard scenario prevails.

4.2. Effectiveness of FD for Dynamically Dissimilar Connected Buildings. The effectiveness of the FDs used to connect the adjacent steel buildings with dissimilar dynamic properties is likewise assessed from the displacement and acceleration responses obtained under the earthquake ground motion and gusty wind excitations. The dissimilarity in their dynamic properties is judged based on the difference in modal properties as well as storey heights of the adjacent steel buildings, such as 5-5 MRF-BF and 5-10 MRF-MRF. Figures 9(a) and 9(b) and Tables 8 and 9 show the peak displacement and acceleration responses of the dynamically dissimilar connected buildings with equal storey height under earthquakes and winds. The peak displacement reduction for the dynamically dissimilar connected buildings with equal storey height is again observed to be the highest for configuration A; however, the range of the difference is significantly large as compared to the dynamically similar buildings of equal storey height.

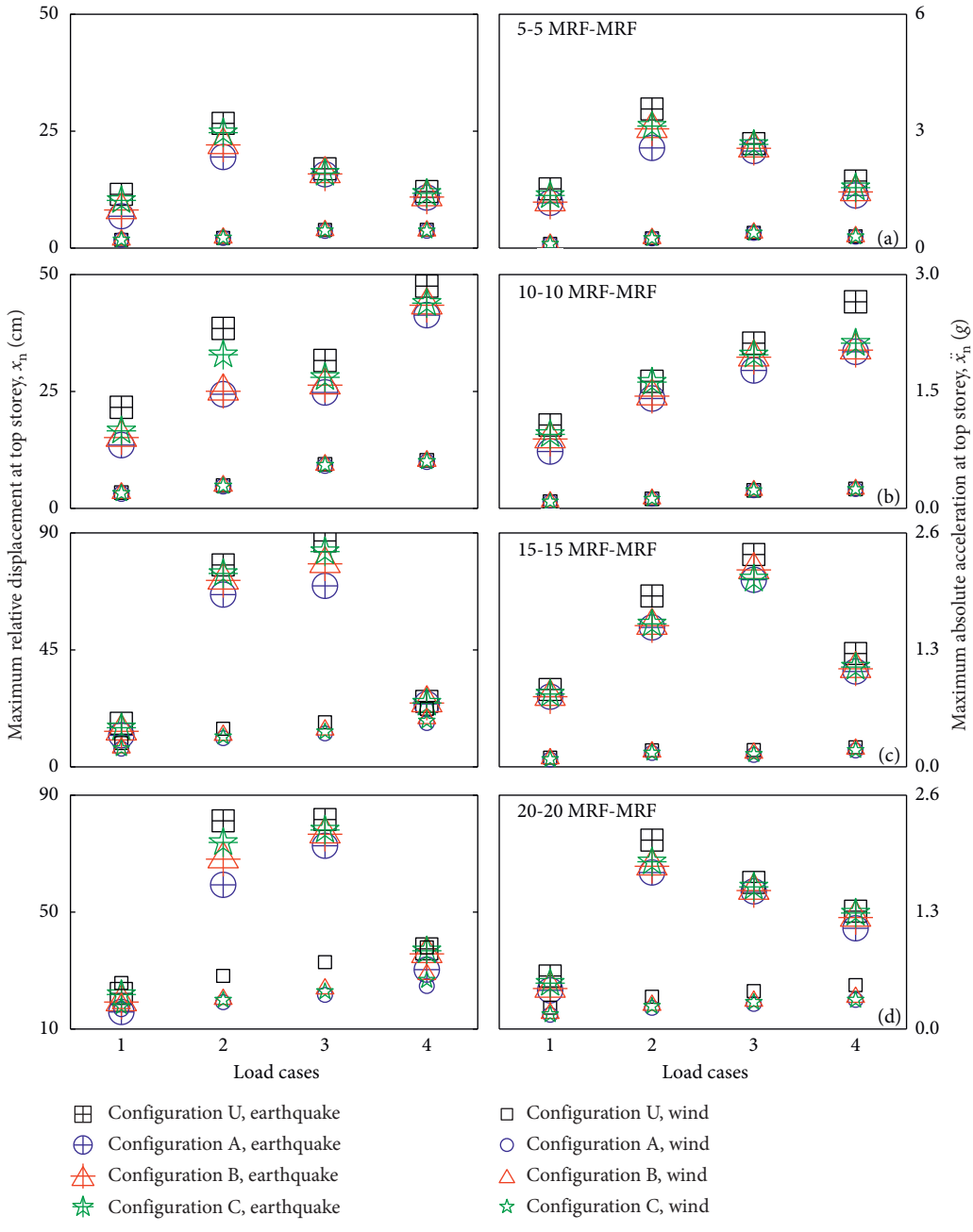

(a)

Figure 8: Continued.

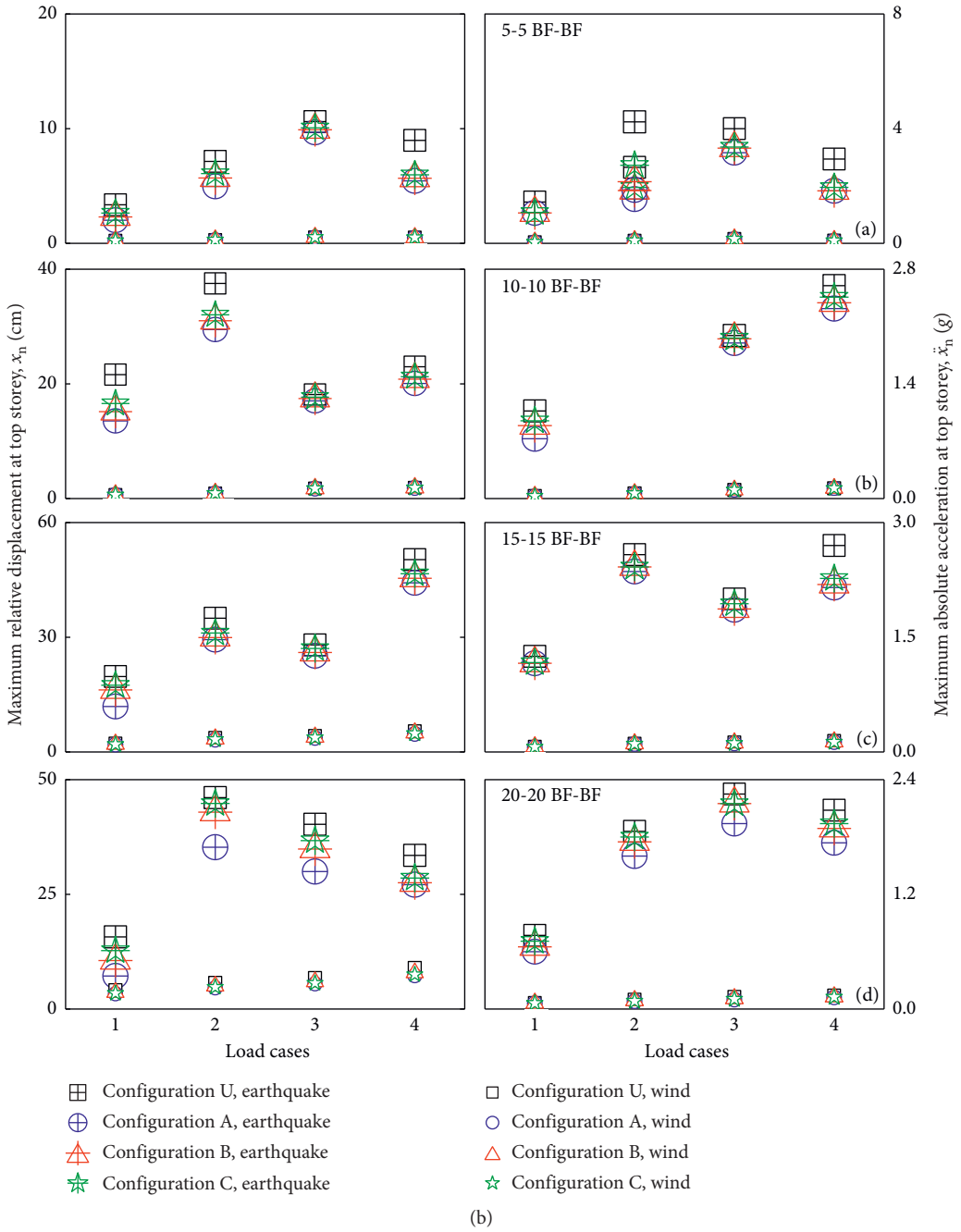

FIGURE 8: (a)Peak top floor displacement and acceleration responses of similar connected MRF-MRF buildings for equal storey height under historical earthquake ground motions and simulated wind forces. (b) Peak top floor displacement and acceleration responses of similar connected BF-BF buildings for equal storey height under historical earthquake ground motions and simulated wind forces.

Considering 5-5 MRF-BF and 5-5 BF-MRF, the displacement response reduction in the first building, i.e., MRF in first case and BF in second case, is observed in the range of ~19% to 80% and ~8% to 40%, respectively. Similarly, for the connected 20-20 MRF-BF and 20-20 BF-MRF, the range of displacement response reduction is also observed to be more for the first MRF building, although the difference in range is relatively lesser as compared to the 5-storey case. This indicates that the BF itself dissipates the earthquake-induced energy even before transferring to the FDs. Under the wind loads, the reduction for the higher number of storey is similarly more as compared to the lower number of storey; however, the range of response reduction is rather negligible. This indicates that the wind force has negligible impact on low-rise building in case of the MRF, and for high-rise BF, the bracings resist the dynamic wind loads, thereby transferring lesser energy to the FDs. Similar observation is made for the peak top floor acceleration responses under both earthquake and wind loadings. Therefore, for the dynamically dissimilar connected buildings with equal storey height,

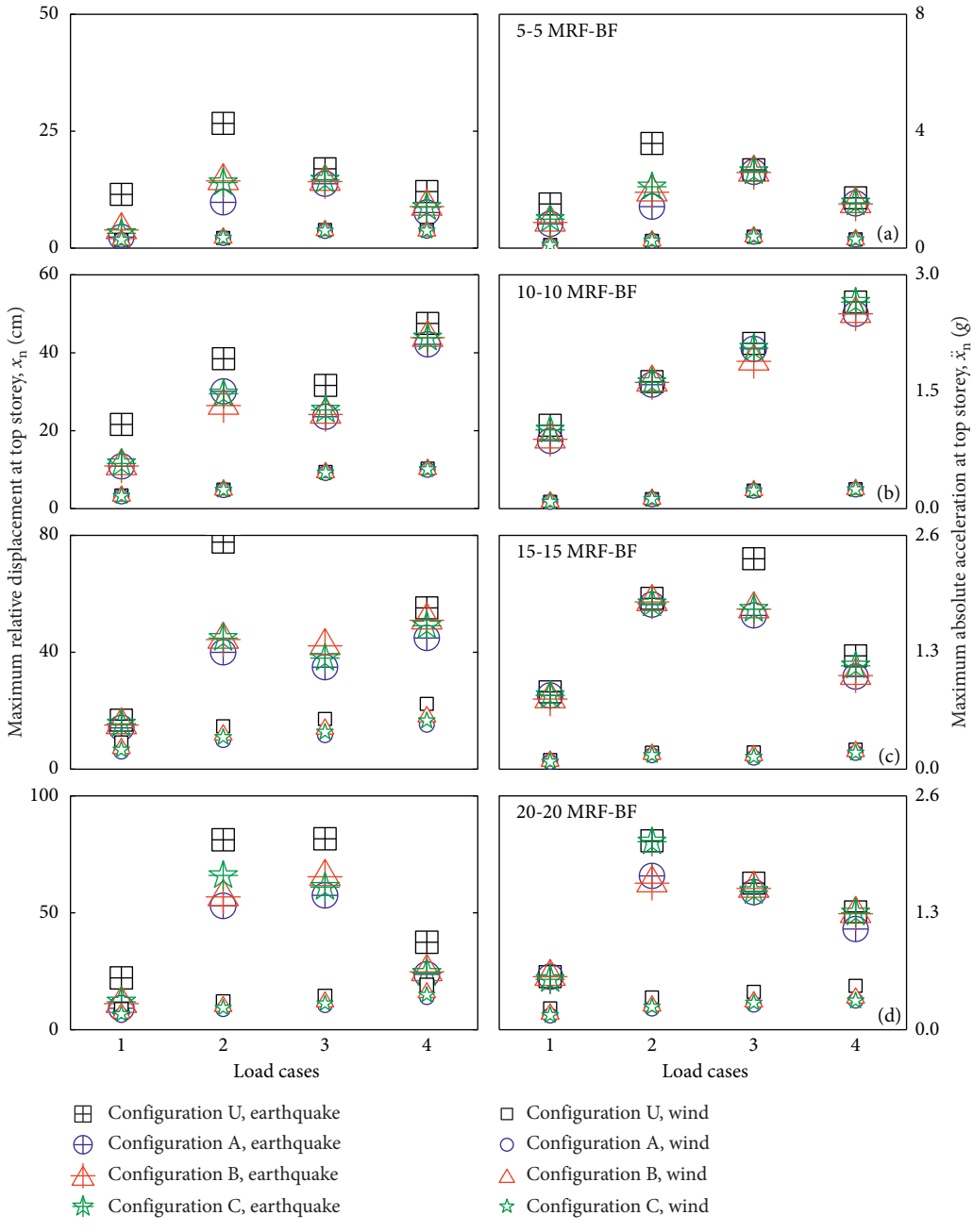

(a)

Figure 9: Continued.

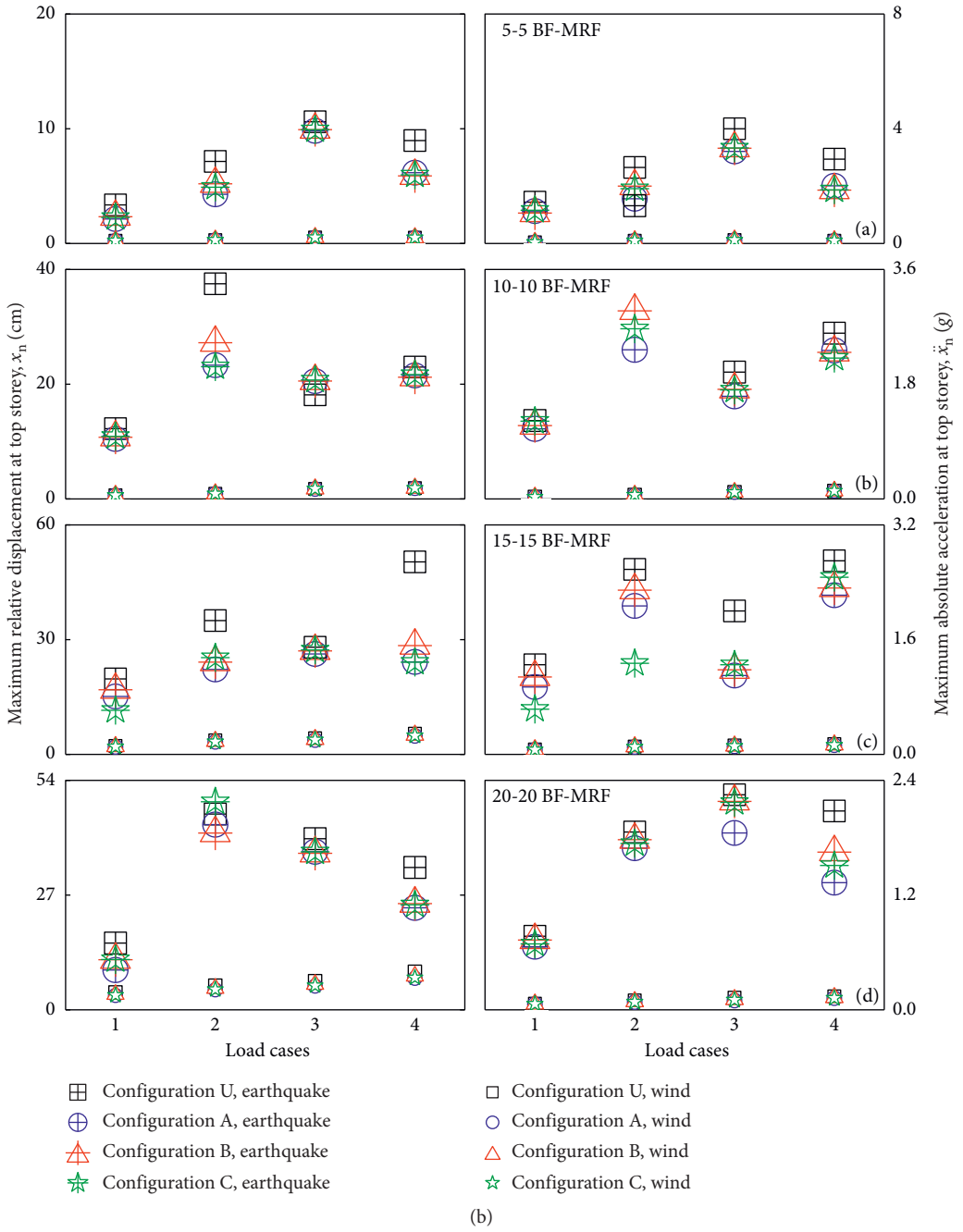

FIGURE 9: (a) Peak top floor displacement and acceleration responses of dissimilar connected MRF-BF buildings for equal storey height under historical earthquake ground motions and simulated wind forces. (b) Peak top floor displacement and acceleration responses of dissimilar connected BF-MRF buildings for equal storey height under historical earthquake ground motions and simulated wind forces.

configuration A serves as an excellent choice for the dynamic response reduction; on the other hand, configuration C is relatively inefficient to reduce the response significantly for dynamically dissimilar connected buildings.

Similarly, the responses for the adjacent steel buildings with dissimilar dynamic properties for unequal storey heights are also quantified under the considered ground motion and gusty wind excitations. Tables 10 and 11 show the peak responses of the first building for the dissimilar connected buildings under the earthquakes and winds, respectively. Figures 10(a) and 10(b) also, respectively, illustrate the displacement and acceleration responses for the adjacent connected MRF and BF steel buildings with unequal storey height under earthquakes and winds. It is observed that the response reduction for the low-rise building (say, 5 storeys) by the FDs is significantly high under the earthquakes as compared to the winds. For the same configuration, the response reduction obtained for the high-rise building (say, 20 storeys) under the winds is substantially higher than the earthquakes as observed

Table 8: Peak top floor displacement and acceleration responses of dissimilar connected buildings for equal storey height under historical earthquake ground motions.

Frame	Earthquake	Peak top floor displacement, x_n (cm)				Peak top floor acceleration, $\ddot{x}_n$ (g)			
		U	A	B	C	U	A	B	C
5-5 MRF-BF	Imperial Valley, 1940	11.49	2.37	3.88	3.17	1.51	0.83	0.88	0.99
	Loma Prieta, 1989	26.67	9.78	14.37	14.02	3.70	1.42	1.91	2.10
	Northridge, 1994	16.96	13.77	14.22	14.58	2.68	2.61	2.59	2.62
	Kobe, 1995	12.10	7.60	8.89	8.74	1.72	1.53	1.51	1.55
20-20 MRF-BF	Imperial Valley, 1940	22.18	9.19	11.17	11.93	0.79	0.79	0.76	0.79
	Loma Prieta, 1989	81.23	52.99	56.80	65.99	2.10	1.71	1.63	2.09
	Northridge, 1994	81.67	57.46	65.42	60.99	1.63	1.53	1.57	1.54
	Kobe, 1995	37.41	23.67	24.76	24.21	1.31	1.12	1.29	1.30
5-5 BF-MRF	Imperial Valley, 1940	3.36	2.13	2.33	2.27	1.44	1.13	1.06	1.16
	Loma Prieta, 1989	7.15	4.28	5.19	4.90	2.65	1.56	2.00	1.91
	Northridge, 1994	10.61	9.81	9.92	9.91	4.00	3.21	3.32	3.33
	Kobe, 1995	8.97	6.17	5.89	5.97	2.94	2.01	1.86	1.87
20-20 BF-MRF	Imperial Valley, 1940	15.72	9.36	11.79	11.84	0.77	0.66	0.73	0.69
	Loma Prieta, 1989	46.08	43.59	41.61	48.97	1.86	1.69	1.78	1.74
	Northridge, 1994	40.27	37.22	36.84	37.18	2.25	1.85	2.18	2.17
	Kobe, 1995	33.50	24.01	25.00	24.72	2.08	1.33	1.65	1.51

Table 9: Peak top floor displacement and acceleration responses of dissimilar connected buildings for equal storey height under simulated wind forces for different gust speeds.

Frame	Wind speed (m/s)	Peak top floor displacement, x_n (cm)				Peak top floor acceleration, $\ddot{x}_n$ (g)			
		U	A	B	C	U	A	B	C
5-5 MRF-BF	30	1.74	1.74	1.74	1.74	0.11	0.097	0.10	0.10
	37	2.16	2.16	2.16	2.16	0.25	0.25	0.25	0.25
	43	3.87	3.65	3.75	3.72	0.39	0.39	0.39	0.39
	50	3.90	3.70	3.69	3.70	0.30	0.29	0.29	0.29
20-20 BF-MRF	30	4.09	3.37	3.62	3.45	0.064	0.059	0.061	0.060
	37	5.69	4.70	5.03	4.80	0.098	0.081	0.086	0.082
	43	6.75	5.58	5.97	5.70	0.13	0.097	0.11	0.10
	50	8.95	7.40	7.92	7.56	0.14	0.12	0.13	0.12

Table 10: Peak top floor displacement and acceleration responses of dissimilar connected buildings for unequal storey height under historical earthquake ground motions.

Frame	Earthquake	Peak top floor displacement, x_n (cm)				Peak top floor acceleration, $\ddot{x}_n$ (g)			
		U	A	B	C	U	A	B	C
5-10 MRF-MRF	Imperial Valley, 1940	11.49	6.43	6.52	8.01	1.51	0.89	0.96	0.92
	Loma Prieta, 1989	26.67	12.86	9.09	11.32	3.58	1.65	1.36	1.85
	Northridge, 1994	16.96	10.43	11.73	12.35	2.68	2.06	2.59	2.08
	Kobe, 1995	12.10	10.47	10.01	11.20	1.72	1.69	1.65	1.58
15-20 MRF-MRF	Imperial Valley, 1940	16.77	10.79	14.82	15.20	0.86	0.65	0.61	0.50
	Loma Prieta, 1989	77.69	59.52	66.83	68.43	1.90	1.53	1.69	1.69
	Northridge, 1994	86.91	67.88	70.78	73.00	2.36	1.24	1.45	1.35
	Kobe, 1995	25.19	22.82	23.13	23.21	1.26	1.14	1.15	1.16
5-10 BF-BF	Imperial Valley, 1940	3.36	2.39	1.86	2.06	1.44	0.89	0.93	0.90
	Loma Prieta, 1989	7.15	3.87	4.10	4.37	2.65	1.08	1.14	1.34
	Northridge, 1994	10.61	7.39	8.46	8.14	4.00	2.44	2.72	2.67
	Kobe, 1995	8.97	3.84	4.64	4.43	2.94	1.43	1.67	1.56
15-20 BF-BF	Imperial Valley, 1940	19.74	6.19	9.11	10.67	1.25	0.85	0.67	1.02
	Loma Prieta, 1989	34.99	27.85	32.11	32.97	2.58	1.58	1.81	1.78
	Northridge, 1994	28.01	25.94	26.94	26.80	2.00	1.86	1.88	1.90
	Kobe, 1995	50.33	31.96	34.88	36.20	2.70	1.81	2.01	1.98

from the difference in the responses from the plots. From the response reductions obtained, configuration A again provides with the most effective option to mitigate the dynamic responses under the earthquakes and winds, whereas the configuration C is apparently the least effective option.

Table 11: Peak top floor displacement and acceleration responses of dissimilar connected buildings for unequal storey height under simulated wind forces for different gust speeds.

Frame	Wind speed (m/s)	Peak top floor displacement, x_n (cm)				Peak top floor acceleration, $\ddot{x}_n$ (g)			
		U	A	B	C	U	A	B	C
5-10 MRF-MRF	30	1.75	0.88	0.88	0.88	0.11	0.08	0.076	0.076
	37	2.17	2.16	2.17	2.17	0.25	0.25	0.25	0.25
	43	3.87	3.83	3.86	3.86	0.39	0.39	0.39	0.39
	50	3.91	3.70	3.72	3.69	0.30	0.29	0.29	0.29
15-20 BF-BF	30	2.20	2.23	2.30	2.26	0.068	0.068	0.071	0.068
	37	3.68	3.56	3.73	3.62	0.11	0.11	0.11	0.11
	43	4.21	4.07	4.25	4.14	0.12	0.11	0.12	0.11
	50	5.41	5.23	5.45	5.31	0.14	0.13	0.14	0.13

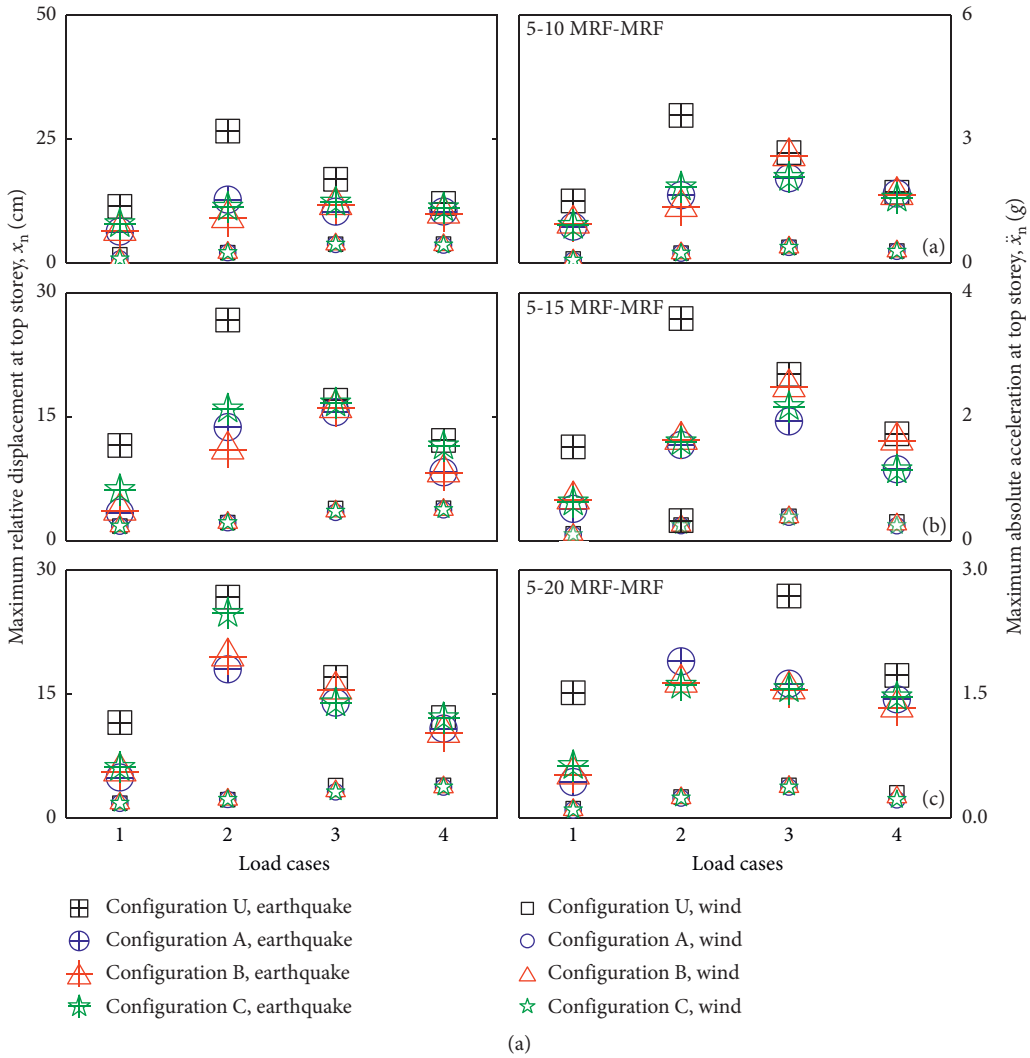

(a)

Figure 10: Continued.

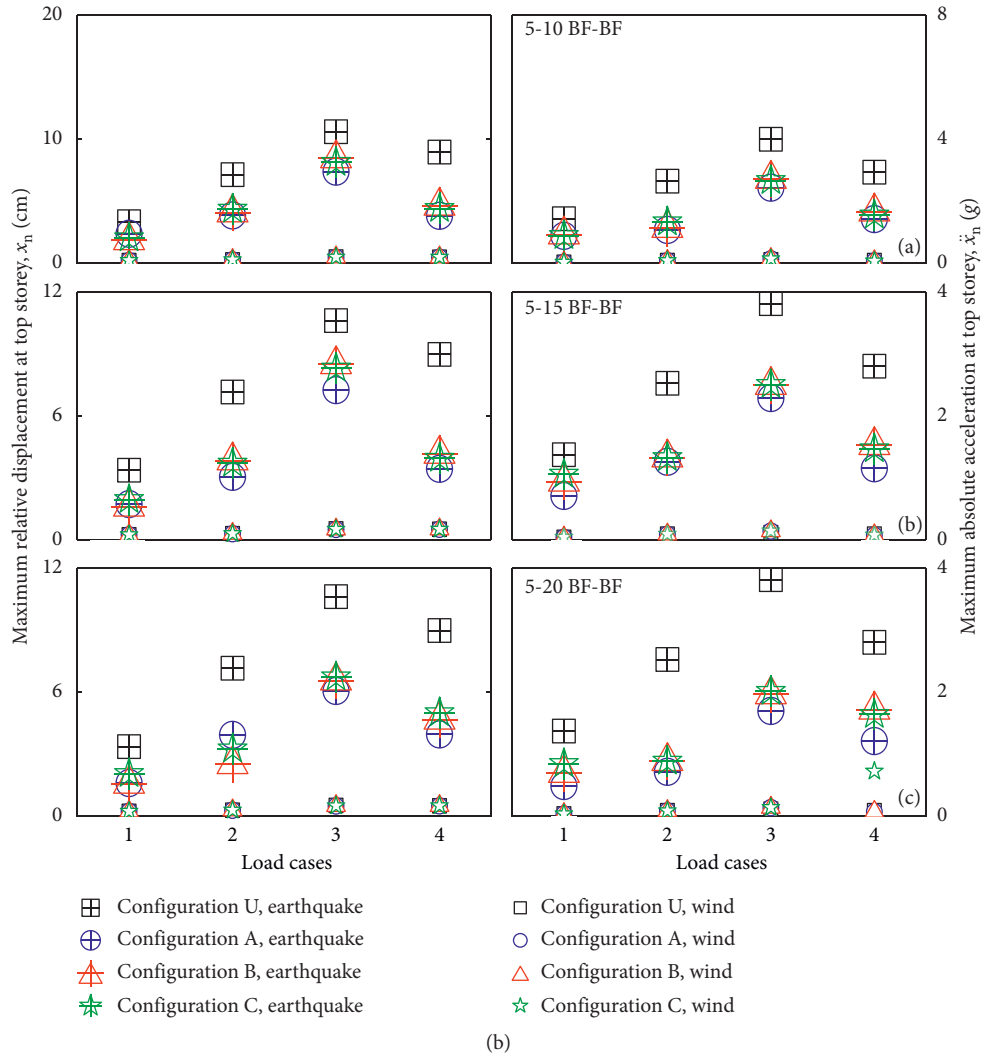

FIGURE 10: (a) Peak top floor displacement and acceleration responses of the adjacent dissimilar connected MRF-MRF buildings with unequal storey height under historical earthquake ground motions and simulated wind forces. (b) Peak top floor displacement and acceleration responses of the adjacent dissimilar connected BF-BF buildings with unequal storey height under historical earthquake ground motions and simulated wind forces.

Table 12 shows the effectiveness of the FDs in terms of average response reduction for the different configurations of the connected dynamically similar and dissimilar steel buildings. Based on the effectiveness achieved, it can be stated that configuration A is best suited to minimize the desired responses under the earthquakes and winds. On the other hand, the least effectiveness is achieved for configuration B for dynamically similar connected buildings and configuration C for dynamically dissimilar connected buildings. Moreover, for limited cases, with increasing the number of storeys, the effectiveness of the dampers increases for high-rise buildings under the wind loadings, becoming almost similar to response reductions under the earthquake loadings. Although the FDs are able to reduce the responses under the earthquakes for higher storeys, the effectiveness of the passive devices is restrained when used in higher stories, demonstrating a need for the multihazard analysis and design under earthquake and wind during design life of the structures. To our belief, there are several structures influenced by the effects of earthquakes and winds, and such structures are required be assessed considering the multihazard effects during their design (service) life. Hence, it can be concluded that the passive FDs are more effective for low-rise buildings under the effect of seismic ground motions, whereas the same control devices show their effectiveness for high-rise buildings under the effect of gusty wind speeds.

As observed from the data, the maximum top floor displacement under the earthquakes for the unconnected MRFs of 5, 10, 15, and 20 storeys are, respectively, obtained as 11.49 cm to 26.67 cm, 21.61 cm to 47.53 cm, 16.77 cm to 86.91 cm, and 22.18 cm to 81.67 cm. Similarly, for the unconnected BFs, the peak displacements, respectively, range from 3.32 cm to 10.32 cm, 11.11 cm to 37.45 cm, 20.13 cm to 49.16 cm, and 15.69 cm to 45.67 cm for increasing height of the buildings. Considering 20-storey building, the minimum separation gap distance required to be kept is ~1.75 m for the

Table 12: Effectiveness of the FDs for different configurations of the connected dynamic similar and dissimilar steel buildings under earthquake ground motions and gust wind speeds.

Frame	Events	Peak top floor displacement, x_n (%)			Peak top floor acceleration, $\ddot{x}_n$ (%)		
		A	B	C	A	B	C
5-5 MRF-MRF	Earthquake	21.33	15.63	6.83	20.07	14.35	8.53
	Wind	2.77	2.12	2.37	3.52	1.97	2.28
20-20 MRF-MRF	Earthquake	21.39	10.02	4.21	16.22	12.10	7.39
	Wind	33.97	26.90	30.15	33.90	26.59	31.28
5-5 BF-BF	Earthquake	29.72	23.82	18.70	31.75	27.92	25.27
	Wind	0.33	0.19	0.24	0.75	0.48	0.75
20-20 BF-BF	Earthquake	20.55	17.70	11.33	26.97	22.14	19.38
	Wind	19.01	11.99	16.45	15.36	9.94	13.20
5-5 MRF-BF	Earthquake	49.65	38.75	40.40	29.75	25.98	21.97
	Wind	2.75	2.08	2.33	3.52	1.86	2.45
20-20 MRF-BF	Earthquake	39.92	33.35	31.39	9.80	6.89	2.96
	Wind	28.28	17.68	22.78	33.90	26.59	31.28
5-5 BF-MRF	Earthquake	29.51	23.10	30.97	28.51	26.16	25.13
	Wind	1.37	0.42	1.37	0.34	0.14	0.24
20-20 BF-MRF	Earthquake	11.45	8.52	10.24	19.32	8.32	11.95
	Wind	17.43	11.52	15.65	15.56	10.28	13.74
5-10 MRF*-MRF	Earthquake	36.95	39.31	30.62	29.96	26.47	29.48
	Wind	14.03	13.64	13.87	8.53	8.07	8.30
15-20 MRF*-MRF	Earthquake	22.59	13.09	11.29	25.22	21.85	25.91
	Wind	20.61	12.36	16.70	12.44	9.56	12.44
5-10 MRF-MRF*	Earthquake	17.91	15.32	12.16	9.75	5.69	2.65
	Wind	14.93	14.63	14.78	2.63	2.14	2.42
15-20 MRF-MRF*	Earthquake	22.93	15.04	8.01	9.85	5.47	−2.94
	Wind	43.90	41.85	44.33	3.74	4.38	3.10

*Response reduction obtained for that building.

unconnected situation. Now, when this 20-storey building is connected by the passive response control devices, FDs, the separation gap distance reduces to minimum ~1.52 m considering the worst case out-of-phase movement at unconnected floors. Hence, there is an opportunity to reduce the separation gap distance by ~30%, thereby constructing buildings at a close vicinity, which would eventually minimize, if not eliminate, structural pounding as well as utilizing the premium space for effective construction.

5. Conclusions

The performance of dynamically similar and dissimilar adjacent steel buildings connected with friction dampers (FDs) is assessed under a set of historical earthquake and simulated wind loadings. The displacement and acceleration responses are compared in order to establish effectiveness of the FDs under the multihazard uncorrelated scenarios of earthquakes and winds. The FDs are capable to reduce the displacement and acceleration responses substantially; however, different configurations are effective under the two hazards for varying building types. This is a concern where the FDs designed for earthquake loading consideration may not necessarily perform better under wind loading. Hence, further investigations are deemed necessary on multihazard analysis and design of the passive response control devices. Nonetheless, from the study conducted herein, the major conclusions drawn are as follows:

(1) The displacement response increases with increase in building height, whereas the acceleration response under the earthquakes decreases with increase in building height for the connected buildings under the seismic ground motions. On the other hand, the dynamic response obtained under the wind loadings generally increases with increase in height of the buildings.

(2) The FDs are more effective in reducing the responses of connected dynamically dissimilar adjacent buildings as compared to the dynamically similar buildings, which is evident from the extent of dynamic response reduction achieved. Moreover, the effectiveness of the FDs has decreased under the earthquakes on increasing the number of stories, whereas their effectiveness substantially increased under the wind loading scenarios.

(3) For the dynamically similar and dissimilar connected buildings, configuration A, with cross-bracing at all floor levels, is most effective in minimizing the responses under seismic and wind excitations, whereas configuration B and C are least effective, respectively, for the dynamically similar and dissimilar connected buildings.

(4) The structures designed to resist the seismic forces in their design (service) life might become vulnerable against the wind loadings. Such structures are required to be assessed and designed carefully to mitigate the responses against the multihazard effects of earthquakes and winds.

Data Availability

All data used to support the findings of the study are included within the article.

Conflicts of Interest

The authors declare that they have no conflicts of interest.

References

[1] S. Chapain and A. M. Aly, "Vibration attenuation in high-rise buildings to achieve system-level performance under multiple hazards," *Engineering Structures*, vol. 197, Article ID 109352, 2019.

[2] S. Elias, "Seismic energy assessment of buildings with tuned vibration absorbers," *Shock and Vibration*, vol. 2018, Article ID 2051687, 2018.

[3] S. Elias, R. Rupakhety, and S. Olafsson, "Analysis of a benchmark building installed with tuned mass dampers under

wind and earthquake loads," *Shock and Vibration*, vol. 2019, Article ID 7091819, 2019.

[4] K. S. Numayr, S. T. Mesmar, and M. A. Haddad, "Dynamic analysis of tapered thin-walled masts," *Journal of Engineering Science and Technology*, vol. 13, no. 7, pp. 2106–2124, 2018.

[5] T. Roy and V. Matsagar, "Effectiveness of passive response control devices in buildings under earthquake and wind during design life," *Structure and Infrastructure Engineering*, vol. 15, no. 2, pp. 252–268, 2019.

[6] T. Roy and V. Matsagar, "Probabilistic assessment of steel buildings installed with passive control devices under multi-hazard scenario of earthquake and wind," *Structural Safety*, vol. 85, Article ID 101955, 2020.

[7] S. Cherry and A. Filiatrault, "Seismic response control of buildings using friction dampers," *Earthquake Spectra*, vol. 9, no. 3, pp. 447–466, 1993.

[8] X. Zhou and L. Peng, "A new type of damper with friction-variable characteristics," *Earthquake Engineering and Engineering Vibration*, vol. 8, no. 4, pp. 507–520, 2010.

[9] B. He, H. Ouyang, S. He, and X. Ren, "Stick-slip vibration of a friction damper for energy dissipation," *Advances in Mechanical Engineering*, vol. 9, no. 7, pp. 1–13, 2017.

[10] L. M. Moreschi and M. P. Singh, "Design of yielding metallic and friction dampers for optimal seismic performance," *Earthquake Engineering & Structural Dynamics*, vol. 32, no. 8, pp. 1291–1311, 2003.

[11] S. Mathur and S. K. Deb, "Seismic response control of RC setback building with friction dampers," *Indian Concrete Journal*, vol. 77, no. 11, pp. 1469–1472, 2003.

[12] Y. L. Xu, W. L. Qu, and Z. H. Chen, "Control of wind-excited truss tower using semiactive friction damper," *Journal of Structural Engineering*, vol. 127, no. 8, pp. 861–868, 2001.

[13] S. Mahmoud, A. Abd-Elhamed, and R. Jankowski, "Earthquake-induced pounding between equal height multi-storey buildings considering soil-structure interaction," *Bulletin of Earthquake Engineering*, vol. 11, no. 4, pp. 1021–1048, 2013.

[14] C. C. Patel and R. S. Jangid, "Seismic response of dynamically similar adjacent structures connected with viscous dampers," *The IES Journal Part A: Civil & Structural Engineering*, vol. 3, no. 1, pp. 1–13, 2009.

[15] A. S. Pall and C. Marsh, "Seismic response of friction damped braced frames," *Journal of Structural Engineering (ASCE)*, vol. 109, no. 5, pp. 1313–1323, 1982.

[16] A. S. Pall, C. Marsh, and P. Fazio, "Friction joints for seismic control of large panel structures," *PCI Journal*, vol. 25, no. 6, pp. 38–61, 1980.

[17] H.-S. Chung, B.-W. Moon, S.-K. Lee, J.-H. Park, and K.-W. Min, "Seismic performance of friction dampers using flexure of RC shear wall system," *The Structural Design of Tall and Special Buildings*, vol. 18, no. 7, pp. 807–822, 2009.

[18] P. Colajanni and M. Papia, "Seismic response of braced frames with and without friction dampers," *Engineering Structures*, vol. 17, no. 2, pp. 129–140, 1995.

[19] A. S. Pall and C. Marsh, "Friction damped concrete shear walls," *American Concrete Institute*, vol. 78, no. 3, pp. 187–193, 1981.

[20] R. Chandra, M. Masand, S. K. Nandi, C. P. Tripathi, R. Pall, and A. Pall, "Friction-dampers for seismic control of la gardenia towers south city, Gurgaon, India," in *12th World Conference On Earthquake Engineering (12WCEE)*, Auckland, New Zealand, November 2000.

[21] I. H. Mualla and B. Belev, "Performance of steel frames with a new friction damper device under earthquake excitation," *Engineering Structures*, vol. 24, no. 3, pp. 365–371, 2002.

[22] S. Bagheri, M. Barghian, F. Saieri, and A. Farzinfar, "U-shaped metallic-yielding damper in building structures: seismic behavior and comparison with a friction damper," *Structures*, vol. 3, pp. 163–171, 2015.

[23] N. Kaur, V. A. Matsagar, and A. K. Nagpal, "Earthquake response of medium-rise to high-rise buildings with friction dampers," *International Journal of High-Rise Buildings*, vol. 1, no. 4, pp. 311–332, 2012.

[24] R. Montuori, E. Nastri, and V. Piluso, "Theory of plastic mechanism control for the seismic design of braced frames equipped with friction dampers," *Mechanics Research Communications*, vol. 58, pp. 112–123, 2014.

[25] N. Fallah and S. Honarparast, "NSGA-II based multi-objective optimization in design of Pall friction dampers," *Journal of Constructional Steel Research*, vol. 89, pp. 75–85, 2013.

[26] L. F. F. Miguel, L. F. F. Miguel, and R. H. Lopez, "Failure probability minimization of buildings through passive friction dampers," *The Structural Design of Tall and Special Buildings*, vol. 25, no. 17, pp. 869–885, 2016.

[27] J. Kim and S. An, "Optimal distribution of friction dampers for seismic retrofit of a reinforced concrete moment frame," *Advances in Structural Engineering*, vol. 20, no. 10, pp. 1523–1539, 2016.

[28] M. Anoushehei, F. Daneshjoo, S. Mahboubi, and S. Khazaeli, "Experimental investigation on hysteretic behavior of rotational friction dampers with new friction materials," *Steel And Composite Structures*, vol. 24, no. 2, pp. 239–248, 2017.

[29] A. Shirkhani, I. H. Mualla, N. Shabakhty, and S. R. Mousavi, "Behavior of steel frames with rotational friction dampers by endurance time method," *Journal of Constructional Steel Research*, vol. 107, pp. 211–222, 2015.

[30] B. Chen, S. Weng, L. Zhi, and D. Li, "Response control of a large transmission tower-line system under seismic excitations using friction dampers," *Advances in Structural Engineering*, vol. 20, no. 8, pp. 1155–1173, 2016.

[31] A. V. Bhaskararao and R. S. Jangid, "Seismic analysis of structures connected with friction dampers," *Engineering Structures*, vol. 28, no. 5, pp. 690–703, 2006.

[32] D. Wang, T. K. T. Tse, Y. Zhou, and Q. Li, "Structural performance and cost analysis of wind-induced vibration control schemes for a real super-tall building," *Structure and Infrastructure Engineering*, vol. 11, no. 8, pp. 990–1011, 2015.

[33] A. V. Bhaskararao and R. S. Jangid, "Seismic response of adjacent buildings connected with friction dampers," *Bulletin of Earthquake Engineering*, vol. 4, no. 1, pp. 43–64, 2006.

[34] F. Fathi and O. Bahar, "Hybrid coupled building control for similar adjacent buildings," *KSCE Journal of Civil Engineering*, vol. 21, no. 1, pp. 265–273, 2017.

[35] Y. Fukumoto and I. Takewaki, "Critical earthquake input energy to connected building structures using impulse input," *Earthquakes and Structures*, vol. 9, no. 6, pp. 1133–1152, 2015.

[36] V. A. Matsagar and R. S. Jangid, "Viscoelastic damper connected to adjacent structures involving seismic isolation," *Journal of Civil Engineering and Management*, vol. 11, no. 4, pp. 309–322, 2005.

[37] V. A. Matsagar and R. S. Jangid, "Base-isolated building connected to adjacent building using viscous dampers," *Bulletin of the New Zealand Society for Earthquake Engineering*, vol. 39, no. 1, pp. 59–80, 2006.

[38] R. Rupakhety, S. Elias, and S. Olafsson, "Shared tuned mass dampers for mitigation of seismic pounding," *Applied Sciences*, vol. 10, no. 6, p. 1918, 2020.

[39] E. Tubaldi, "Dynamic behavior of adjacent buildings connected by linear viscous/viscoelastic dampers," *Structural*

Control and Health Monitoring, vol. 22, no. 8, pp. 1086–1102, 2015.

[40] T. Roy and V. Matsagar, "Multi-hazard assessment of steel buildings retrofitted with passive control devices," in *16th World Conference On Earthquake Engineering (16WCEE)*, Santiago, Chile, January 2017.

[41] D. Kwon and A. Kareem, *NatHaz On-Line Wind Simulator (NOWS): Simulation of Gaussian Multivariate Wind Fields*, University of Notre Dame, Notre Dame, IN, USA, 2006.